VIP Solar Cells Very Important Paper

DOI: 10.1002/ange.201404973

Integrating Perovskite Solar Cells into a Flexible Fiber**

*Longbin Qiu, Jue Deng, Xin Lu, Zhibin Yang, and Huisheng Peng**

Abstract: *Perovskite solar cells have triggered a rapid development of new photovoltaic devices because of high energy conversion efficiencies and their all-solid-state structures. To this end, they are particularly useful for various wearable and portable electronic devices. Perovskite solar cells with a flexible fiber structure were now prepared for the first time by continuously winding an aligned multiwalled carbon nanotube sheet electrode onto a fiber electrode; photoactive perovskite materials were incorporated in between them through a solution process. The fiber-shaped perovskite solar cell exhibits an energy conversion efficiency of 3.3 %, which remained stable on bending. The perovskite solar cell fibers may be woven into electronic textiles for large-scale application by well-developed textile technologies.*

Perovskite materials with the formula $CH_3NH_3PbX_3$ (X = Cl, Br, I) have been known for several decades and have recently attracted increasing attention because of their promising applicability in photovoltaics.[1–3] A typical perovskite solar cell is composed of an n-type compact layer that blocks short circuits, a mesoporous TiO_2 nanocrystal layer, a light-harvesting perovskite layer, a hole-transport layer, and two electrodes. The perovskite layer absorbs light to generate charges that are driven to be separated and transported by the built-in electric field between the two electrodes; this is followed by injection of the electrons into the conduction band of the TiO_2 layer and of the holes into the hole-transport layer; they are then collected by the electrodes.[4,5] Perovskite solar cells exhibit high energy conversion efficiencies of up to 16 %, which are much higher than those of polymer solar cells.[6–8] Furthermore, an all-solid-state structure is produced with high environmental stability, which is particularly important for high-performance flexible devices.[9,10] Indeed, flexible perovskite solar cells with high energy conversion efficiencies, for example, 10.2 %, have recently been reported.[11,12]

On the other hand, wearable and portable devices represent a new and important direction in modern electronics.[13,14] In particular, electronic textiles are highly desired in many fields, such as sensing electronic skins. To this end, it is necessary to integrate efficient power systems that are lightweight and may be woven into flexible materials. Some attempts have recently been made to develop coaxial one-dimensional dye-sensitized and polymer solar cells to meet the advancement in the field of wearable and portable electronics.[15,16] However, liquid electrolytes are generally required for dye-sensitized solar cells, but they display low stabilities. Although eutectic melts can be used as electrolytes to make quasi-solid-state devices with improved stabilities, they suffered from low energy conversion efficiencies (2.6 %).[17] Low energy conversion efficiencies, such as 2.3 %, were also measured for polymer solar cells.[18,19] To the best of our knowledge, no fiber-shaped perovskite solar cells have been reported.

Herein, a novel coaxial fiber-shaped perovskite solar cell with high flexibility and low cost is developed. During a typical fabrication process, a stainless steel fiber with a compact blocking layer was used as the anode, and a perovskite $CH_3NH_3PbI_3$ sensitizer is then coated onto the fiber anode, followed by coating of the hole-transport material and winding of transparent carbon nanotube (CNT) sheets as the cathode (Figure 1a). This all-solid-state fiber-shaped solar cell exhibits an energy conversion efficiency of 3.3 % and can further be woven into flexible perovskite solar cell textiles.

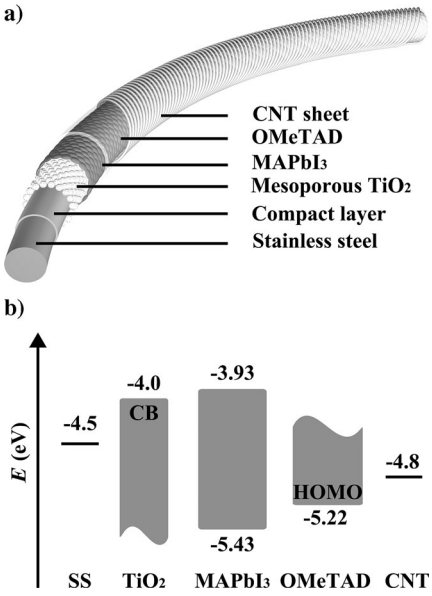

Figure 1. a) Structure and b) energy-level diagram of the fiber-shaped perovskite solar cell. $MAPbI_3 = CH_3NH_3PbI_3$, OMeTAD = 2,2′,7,7′-tetrakis(*N*,*N*-di-*para*-methoxyphenyl-amine)-9,9-spirobifluorene.

[*] L. Qiu,[+] J. Deng,[+] X. Lu, Z. Yang, Prof. H. Peng
State Key Laboratory of Molecular Engineering of Polymers
Department of Macromolecular Science and Laboratory of Advanced Materials, Fudan University
Shanghai 200438 (China)
E-mail: penghs@fudan.edu.cn

[+] These authors contributed equally to this work.

[**] This work was supported by MOST (2011CB932503), the NSFC (21225417), STCSM (12nm0503200), the Fok Ying Tong Education Foundation, the Program for Special Appointments of Professors at Shanghai Institutions of Higher Learning, and the Program for Outstanding Young Scholars from the Organization Department of the CPC Central Committee.

Supporting information for this article is available on the WWW under http://dx.doi.org/10.1002/anie.201404973.

The synthesis of $CH_3NH_3PbI_3$ is described in the Supporting Information; it was further processed into thin films for characterization by spin-coating a $CH_3NH_3PbI_3$/γ-butyrolactone solution onto glass slides, followed by drying at 100 °C, with a chromatic transition from light yellow to dark brown (indicating the formation of the perovskite film). The structure was studied by X-ray diffraction (Supporting Information, Figure S1), and four strong characteristic peaks at 14.08°, 28.40°, 31.84°, and 43.21°, which correspond to the (110), (220), (310), and (330) diffraction peaks, indicate that an orthorhombic crystal has been formed. The extremely narrow diffraction peaks also suggest a long-range crystalline domain.[20,21] The UV/Vis absorption spectra further demonstrate a high light-harvesting capability spanning the visible to the near-infrared spectrum (Figure S2).

The layered structure of the fiber-shaped perovskite solar cell is schematically shown in Figure 1 a. Photoactive layers were then sequentially dip-coated onto the outer surface according to Figure 1 a. Figure 2 and Figure 3 show the

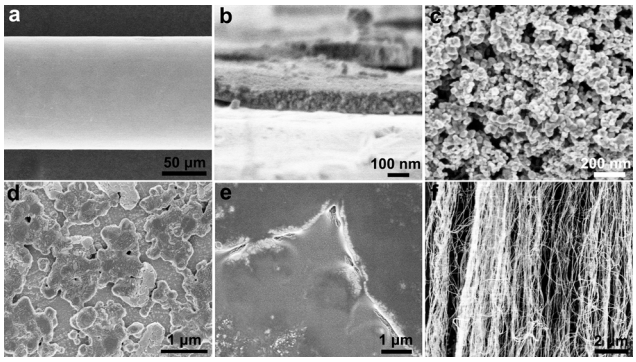

Figure 2. SEM images of the coated layers during the fabrication of the fiber-shaped perovskite solar cell. a) Stainless steel. b) Compact TiO_2 layer. c) Mesoporous TiO_2 crystal layer. d) Perovskite $CH_3NH_3PbI_3$ layer. e) Hole-transport layer. f) CNT sheet.

structure of each layer as it was observed by scanning electron microscopy (SEM). As expected, the outer surface of the steel wire is smooth (Figure 2 a), which is critical for the following uniform deposition of the photoactive material. A thin n-type compact layer was uniformly deposited on the steel wire (Figure 2 b). A mesoporous nanocrystal TiO_2 layer is then deposited to provide a high surface area for the following $CH_3NH_3PbI_3$ deposition (Figure 2 c). The $CH_3NH_3PbI_3$ perovskite layer is further coated onto the nanocrystal TiO_2 layer (Figure 2 d), and the $CH_3NH_3PbI_3$ material could be effectively infiltrated into the mesopore of the nanocrystal layer. It would be difficult to deposit a uniform and dense layer of the $CH_3NH_3PbI_3$ perovskite material without the mesoporous TiO_2 layer. The hole-transport layer was subsequently coated on top of the $CH_3NH_3PbI_3$ layer (Figure 2 e). A transparent CNT sheet that had been dry-drawn from a spinnable CNT array was finally wound onto the outer surface as the cathode (Figure 2 f). Multiwalled CNTs with an average diameter of 10 nm were used. Figure 3 shows a cross-sectional SEM image of the coaxial fiber-shaped solar cell. The thickness of the perov-

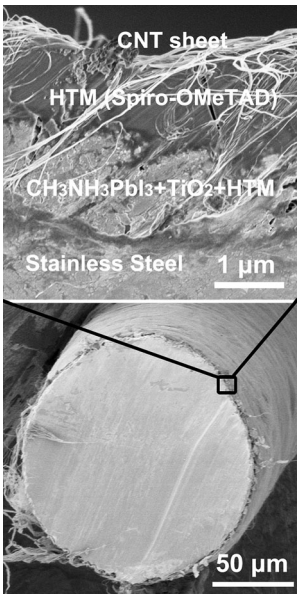

Figure 3. Cross-sectional SEM image of a fiber-shaped perovskite solar cell.

skite-coated mesoporous TiO_2 layer is approximately 1 μm, and the CNT sheet exhibits an average thickness of 20 nm.

The compact TiO_2 layer is used to separate the stainless steel fiber and the hole-transport layer to prevent the recombination of electrons in the stainless steel wire and of holes in the hole-transport layer.[22] Compact TiO_2 layers with a range of thicknesses were prepared by varying the concentration of the TiO_2 precursor solution and by repeatedly dip-coating them onto the steel wire. For the resulting fiber-shaped solar cells with increasing thickness of the compact TiO_2 layer from 25 to 100 nm, J–V curves were recorded under otherwise identical conditions (Figure 4 a). A thicker layer leads to an increase in the series resistance, which produces a lower fill factor (FF); the short-circuit current density decreases with increasing thickness of compact layer. Furthermore, thicker films became fragile and easily broke into many stacked pieces. Therefore, the steel wire and the hole-transport layer were not effectively separated, and a short circuit occurred (Figure S3). On the other hand, it is challenging to obtain very thin, yet continuous films because of the unavoidable existence of defects, which may also result in a short circuit. A solar cell with a compact TiO_2 layer with an optimized thickness of 50 nm was mainly investigated in the following studies.

A series of fiber-shaped perovskite solar cells were fabricated by varying the annealing temperature, and the photovoltaic performances of the resulting devices were measured. The performances of fiber-shaped solar cells annealed at temperatures from 350 to 500 °C are compared in Figure 4 b. A higher annealing temperature favored the formation of a crystal n-type compact TiO_2 layer with higher efficiency, while possibly producing more iron oxide to decrease efficient electron transport.[23] As a result, the maximal energy conversion efficiency was observed for the solar cell annealed at 400 °C (Figure 4 b).

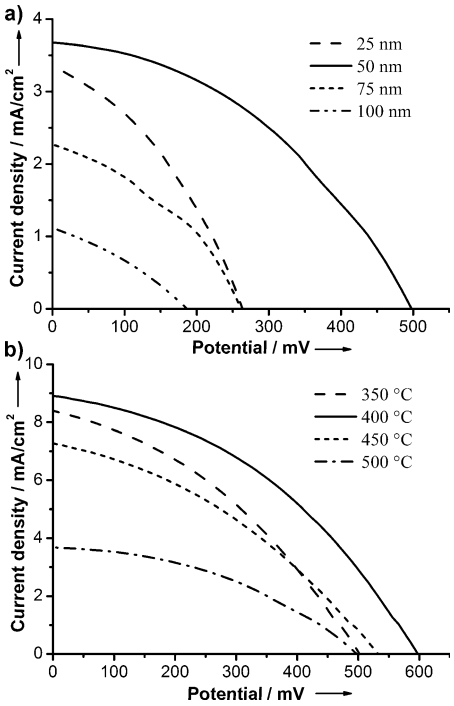

Figure 4. *J–V* curves of fiber-shaped perovskite solar cells with a) different thicknesses of the n-type compact TiO_2 layer and with b) different annealing temperatures.

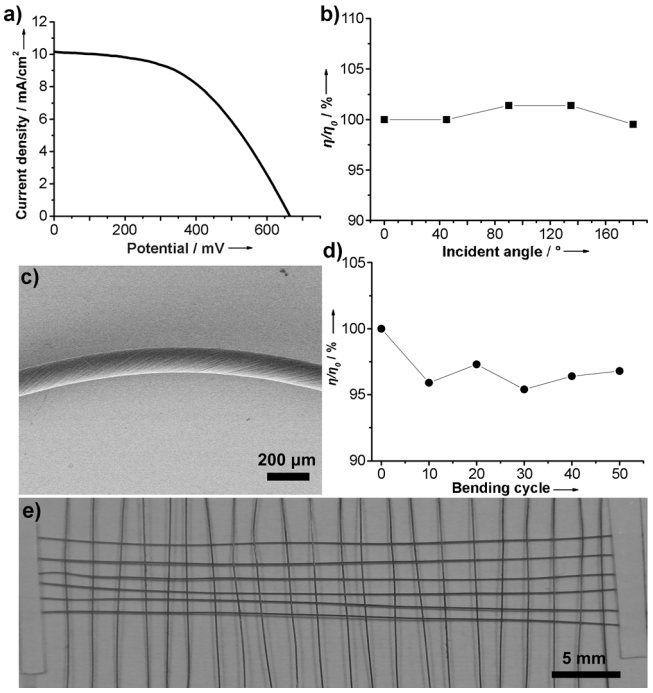

Figure 5. a) *J–V* curve of a coaxial fiber-shaped perovskite solar cell with an energy conversion efficiency of 3.3% (V_{OC} = 0.664 V, I_{SC} = 10.2 mA cm^{-2}, FF = 0.487). b) Dependence of the energy conversion efficiency on the angle of incident light. Here, η_0 and η correspond to the energy conversion efficiencies at 0° and the other angle, respectively. c) SEM image of a bent fiber-shaped perovskite solar cell. d) Dependence of the energy conversion efficiency on the bending-cycle number. Here, η_0 and η correspond to the energy conversion efficiencies before and after bending, respectively. e) Photograph of a textile.

The mesoporous layer greatly improves the light absorbance. The UV/Vis spectra of the perovskite $CH_3NH_3PbI_3$ layers that were deposited on glass slides without and with the mesoporous TiO_2 layer are shown in Figure S2. Figure S4 compares the performance of two fiber-shaped solar cells without and with the mesoporous TiO_2 layer. The short-circuit current density is nearly two times larger with the mesoporous layer than without the mesoporous layer. The generated charges can be more easily recombined without the mesoporous TiO_2 layer, which decreases both the open-circuit voltage (V_{OC}) and the short-circuit current density (J_{SC}).

After optimization, the coaxial fiber-shaped perovskite solar cell currently achieves an energy conversion efficiency of 3.3% (Figure 5a), which exceeds that of other coaxial fiber-shaped dye-sensitized or polymer solar cells.[17–19] As expected, because of the symmetric coaxial structure, the photovoltaic parameters, including V_{OC}, J_{SC}, and FF, remain almost unchanged with an increase in the angle of the incident light from 0 to 180° under the same light intensity (Figure 5b). In other words, the energy conversion efficiencies are independent of the incident angle. These coaxial fiber-shaped perovskite solar cells are flexible and can be bent into various shapes without fatigue (Figure 5c; see also Figure S5). No obvious damages were observed by SEM during bending, and the energy conversion efficiencies remained at 95% after bending for 50 cycles (Figure 5d).

The high photovoltaic performance of the fiber-shaped perovskite solar cell is described below (based on the energy level diagram in Figure 1b). The photo-generated charges from the perovskite layer are separated and transported to the external electric circuit through an efficient built-in electric field between the steel wire and the CNT sheet electrodes. The high surface area and high electrical conductivity of the CNT sheet favor rapid charge transport and collection with high photoelectric currents (Figure S6); the perovskite material exhibits a high molar extinction coefficient,[24] ambipolar behavior,[25] and long-range electron/hole diffusion.[26] Therefore, the resulting fiber-shaped photovoltaic device achieves a high energy conversion efficiency.

In summary, a novel fiber-shaped perovskite solar cell has been synthesized through an easy dip-coating process. Its energy conversion efficiency of 3.3% is the highest that has been reported for coaxial all-solid-state fiber-shaped solar cells. The prepared fiber-shaped solar cells are flexible and can be woven into various structures, such as self-powering textiles (Figure 5e), which are urgently required for miniature electronic devices. A lot of efforts are currently directed towards further increasing the energy conversion efficiency of this solar cell, so that it may meet the practical requirements for such fiber-shaped photovoltaic devices.

Experimental Section

Fiber-shaped perovskite solar cells were fabricated on stainless steel wires with a diameter of 127 μm. Steel wires were first cleaned sequentially in acetone, isopropanol, and deionized water in an

ultrasonic bath for 10 min. The resulting dry steel wire was dip-coated in a diluted titanium diisopropoxide bis(acetylacetonate) solution and dried at 125 °C. The thickness could be increased by repeating the coating process. The coated steel wire was further annealed at 400 °C for 15 min in air and then immersed in an aqueous solution of $TiCl_4$ (40 mM) for 30 min at 70 °C, followed by washing with deionized water and ethanol and annealing at 400 °C for 30 min to form an n-type compact TiO_2 layer. A commercial TiO_2 nanoparticle (diameter: 20 nm) paste (DHS-TPP3, Heptachroma) was diluted with ethanol (1:3 w/w) and then deposited to form the mesoporous TiO_2 layer. After drying at 120 °C, the TiO_2 layers were gradually heated to 400 °C and baked for 30 min. The resulting steel wire was dipped into a perovskite precursor solution, followed by annealing at 100 °C for 10 min in air. A HTM solution containing 2,2′,7,7′-tetrakis(*N*,*N*-di-*para*-methoxyphenyl-amine)-9,9-spirobifluorene (61.4 mM), lithium bis(trifluoromethylsulfonyl)imide (26 mM), and 4-*tert*-butylpyridine (55 mM) in a solvent mixture of chlorobenzene and acetonitrile (20:1 v/v) was coated onto the perovskite layer. An aligned CNT sheet was finally wrapped around the steel wire to produce the fiber-shaped perovskite solar cell.[27,28]

Received: May 5, 2014
Published online: July 22, 2014

Keywords: carbon-based materials · energy conversion · nanotubes · perovskite phases · solar cells

[1] S. Kazim, M. K. Nazeeruddin, M. Grätzel, S. Ahmad, *Angew. Chem.* **2014**, *126*, 2854 – 2867; *Angew. Chem. Int. Ed.* **2014**, *53*, 2812 – 2824.
[2] B. V. Lotsch, *Angew. Chem.* **2014**, *126*, 647 – 649; *Angew. Chem. Int. Ed.* **2014**, *53*, 635 – 637.
[3] H. J. Snaith, *J. Phys. Chem. Lett.* **2013**, *4*, 3623 – 3630.
[4] H. S. Kim, C. R. Lee, J. H. Im, K. B. Lee, T. Moehl, A. Marchioro, S. J. Moon, R. Humphry-Baker, J. H. Yum, J. E. Moser, M. Grätzel, N. G. Park, *Sci. Rep.* **2012**, *2*, 591.
[5] A. Marchioro, J. Teuscher, D. Friedrich, M. Kunst, R. van de Krol, T. Moehl, M. Grätzel, J. E. Moser, *Nat. Photonics* **2014**, *8*, 250 – 255.
[6] J. T. Wang, J. M. Ball, E. M. Barea, A. Abate, J. A. Alexander-Webber, J. Huang, M. Saliba, I. Mora-Sero, J. Bisquert, H. J. Snaith, R. J. Nicholas, *Nano Lett.* **2014**, *14*, 724 – 730.
[7] J. You, L. Dou, K. Yoshimura, T. Kato, K. Ohya, T. Moriarty, K. Emery, C. C. Chen, J. Gao, G. Li, Y. Yang, *Nat. Commun.* **2013**, *4*, 1446.
[8] M. Liu, M. B. Johnston, H. J. Snaith, *Nature* **2013**, *501*, 395 – 398.
[9] S. K. Pathak, A. Abate, T. Leijtens, D. J. Hollman, J. Teuscher, L. Pazos, P. Docampo, U. Steiner, H. J. Snaith, *Adv. Energy Mater.* **2014**, DOI: 10.1002/aenm.201301667.
[10] J. Burschka, N. Pellet, S. J. Moon, R. Humphry-Baker, P. Gao, M. K. Nazeeruddin, M. Grätzel, *Nature* **2013**, *499*, 316 – 319.
[11] D. Y. Liu, T. L. Kelly, *Nat. Photonics* **2014**, *8*, 133 – 138.
[12] J. You, Z. Hong, Y. M. Yang, Q. Chen, M. Cai, T. B. Song, C. C. Chen, S. Lu, Y. Liu, H. Zhou, Y. Yang, *ACS Nano* **2014**, *8*, 1674 – 1680.
[13] T. Chen, Z. Yang, H. Peng, *ChemPhysChem* **2013**, *14*, 1777 – 1782.
[14] T. Chen, L. Qiu, Z. Yang, H. Peng, *Chem. Soc. Rev.* **2013**, *42*, 5031 – 5041.
[15] H. Sun, X. You, Z. Yang, J. Deng, H. Peng, *J. Mater. Chem. A* **2013**, *1*, 12422.
[16] B. O'Connor, K. P. Pipe, M. Shtein, *Appl. Phys. Lett.* **2008**, *92*, 193306.
[17] H. Sun, H. Li, X. You, Z. Yang, J. Deng, L. Qiu, H. Peng, *J. Mater. Chem. A* **2014**, *2*, 345.
[18] D. Liu, M. Zhao, Y. Li, Z. Bian, L. Zhang, Y. Shang, X. Xia, S. Zhang, D. Yun, Z. Liu, A. Cao, C. Huang, *ACS Nano* **2012**, *6*, 11027 – 11034.
[19] Z. Zhang, X. Chen, P. Chen, G. Guan, L. Qiu, H. Lin, Z. Yang, W. Bai, Y. Luo, H. Peng, *Adv. Mater.* **2014**, *26*, 466 – 470.
[20] T. Baikie, Y. Fang, J. M. Kadro, M. Schreyer, F. Wei, S. G. Mhaisalkar, M. Grätzel, T. J. White, *J. Mater. Chem. A* **2013**, *1*, 5628.
[21] Q. Chen, H. Zhou, Z. Hong, S. Luo, H. S. Duan, H. H. Wang, Y. Liu, G. Li, Y. Yang, *J. Am. Chem. Soc.* **2014**, *136*, 622 – 625.
[22] J. H. Yum, P. Chen, M. Grätzel, M. K. Nazeeruddin, *ChemSusChem* **2008**, *1*, 699 – 707.
[23] Y. Zhu, L. Zhang, L. Wang, Y. Fu, L. Cao, *J. Mater. Chem.* **2001**, *11*, 1864 – 1868.
[24] L. Etgar, P. Gao, Z. Xue, Q. Peng, A. K. Chandiran, B. Liu, M. K. Nazeeruddin, M. Grätzel, *J. Am. Chem. Soc.* **2012**, *134*, 17396 – 17399.
[25] J. Shi, J. Dong, S. Lv, Y. Xu, L. Zhu, J. Xiao, X. Xu, H. Wu, D. Li, Y. Luo, Q. Meng, *Appl. Phys. Lett.* **2014**, *104*, 063901.
[26] G. Xing, N. Mathews, S. Sun, S. S. Lim, Y. M. Lam, M. Grätzel, S. Mhaisalkar, T. C. Sum, *Science* **2013**, *342*, 344 – 347.
[27] L. Qiu, X. Sun, Z. Yang, W. Guo, H. Peng, *Acta Chim. Sin.* **2012**, *70*, 1523.
[28] Z. Yang, J. Deng, X. Sun, H. Li, H. Peng, *Adv. Mater.* **2014**, *26*, 2643 – 2647.